Figure 2.4 Sediment transport patterns based on modeled flow patterns, imagery, and existing literature.

2.2 Merrimack River Inlet Dredging

The Merrimack River Inlet is a federally maintained inlet that is periodically dredged by USACE. Detailed dredging records at the Merrimack River extend back to 1961. The average volume dredged per year between 1961 and 2010 is 38,000 cubic yards (Table 2.1). For the first 20 years of dredging, the sediment was disposed of at an offshore location 1-2 miles from the inlet. Beginning in the early 1980's through 1999, dredging spoils were disposed of at a nearshore disposal site along the bypass bar. Over

this 20-year period, close to one million cubic yards were placed along the bypass bar. Although, this placement provided wave protection for the northern end of Plum Island, the bolstering of the bar may have amplified currents moving alongshore between the bar and shoreline. More recently, spoils from the 2010 dredging of the inlet were placed onshore in both Salisbury and Plum Island. This placement provided sediment directly to the littoral system for both beaches and acted as a buffer for the shoreline near Center Island Groin. However, this buffer was short lived, indicating a possible need for more frequent nourishment to mitigate the erosion hotspot formation. Nourishment options are described in Sections 5 and 6.

Since long-term erosion rates are rather modest for the overall shoreline adjacent to the Merrimack River entrance, with the exception of the erosional “hot spot” along Plum Island, the volume of sand needed to maintain the shoreline position can be managed with material from the inlet, removed on an annual basis. In general, the 38,000 cubic yards removed from the inlet on an annual basis could supply enough sediment to stabilize between 4,000 and 8,000 feet of shoreline if it was placed directly on the beach. To increase placement efficiency as mobilization of dredging equipment is expensive, the material could be placed in recurring intervals at locations both on Plum Island and Salisbury Beach. Realistically, this dredging would occur on a three to five-year interval, similar to dredging frequencies between 1960 and 1999, rather than on an annual basis, to reduce mobilization costs. Therefore, supplemental volumes may be required to properly nourish the erosion hotspot. Additional sediment sources are discussed in Section 6.1.

Table 2.1 Maintenance dredging history in the Merrimack River Inlet

Date Completed (Month, Year)	Volume (cubic yards)	
August, 1961	250,000	Offshore Placement
May, 1964	131,000	Offshore Placement
May, 1966	50,000	Offshore Placement
July, 1968	86,000	Offshore Placement
July, 1970	106,190	Offshore Placement
October, 1970	183,230	Offshore Placement
September, 1973	93,650	Offshore Placement
July, 1977	54,000	Offshore Placement
July, 1981	102,600	Nearshore Bypass Bar
August, 1983	123,500	Nearshore Bypass Bar
September, 1983	154,000	Nearshore Bypass Bar
September, 1991	135,290	Nearshore Bypass Bar
May, 1993	125,040	Nearshore Bypass Bar
September, 1996	125,386	Nearshore Bypass Bar
August, 1999	145,017	Nearshore Bypass Bar
October, 2010	160,000	Onshore
Average	38,000 (per year)	
Total	1,899,863	

2.3 Engineering Management Responses

Following their completion in 1914 (1905 for the south jetty), the Merrimack River inlet jetties have been rehabilitated several times, only to destabilize over time. There are three distinct rehabilitation periods in the jetties' history: 1934 to 1938, 1966 to 1969, and 2013 to 2015. Following rehabilitation, the structural integrity of the jetties begins to degrade as storms erode sediment along the toe of the structure. The jetty condition continues to deteriorate until they are repaired and refurnished with stone. The condition of the jetties has a profound impact on flow passing from the east-facing Plum Island Beach and Reservation Terrace.

The inlet is routinely dredged every 3 to 5 years, but has been on the order of every 10 years recently. Typical dredging volumes are between 150,000 and 200,000 cubic yards. The formation and characteristics of the ebb tidal delta have been cited as evidence of sediment being derived from the Merrimack River itself, rather than from littoral sources (Fallon, 2016).

There are many historical USACE reports that date back to the 1800's for both north and south of the inlet. These reports range from dredging, structural maintenance, to management recommendations For example, a beach erosion control report from 1952 recommended local interests to take on protective measures, because the shoreline was private at the time (Wentworth, 1969). It wasn't until the 2010 beach nourishment that an easement along Plum Island Beach was secured, allowing dredged material to be placed onshore to build a berm.

In the past two years, there have been several coastal processes and management studies completed. In 2017, Woods Hole Group released a Marsh Resiliency Study which examined coastal processes in the region to quantify the rate and direction of sediment flux along the shoreline for average-annual and storm conditions. The study determined that a divergence in sediment transport occurs that migrates depending on wave direction. These results lacked meaningful implications as the divergent transport along Plum Island Beach location has been documented previously, and it is well understood that nodal points along the beach associated with alongshore sediment transport will change depending on the average incident wave direction. Also, the rate of sediment transport potential presented was a single value of 72,000 cubic yards per year to the south. This value includes no spatial variability in the alongshore direction, which clearly is not the case. Further, the sediment transport evaluation included in this study provided no calibration or validation information; therefore, the provided sediment transport rates represent strictly numerical modeling estimates.

In June 2018 ERDC performed a similar coastal processes study that included a comprehensive alternatives analysis with 24 total alternatives (Li et al., 2018). Although the study was complete in testing many alternatives, many of the results were not practicable, leaving out environmental concerns and recommending unrealistic options from an environmental permitting perspective. For example, one alternative recommends dredging of over 500,000 cubic yards from within the estuary. Although USACE concludes there will be minimal implications to the resultant flow and sediment transport patterns, there would likely be significant environmental concerns. Also, recommendations are made to modify the bypass bar by either dredging similar volumes or filling in bar breaks. Although the alteration of the ebb shoal might provide protection for some parts of the beach, the bar is critical in protecting the northern end of Plum Island from storm waves. Careful consideration of some of these impacts is critical to the consideration of shore protection alternatives. A review of relevant historical scientific analyses and literature to the project area is also important to developing and testing alternatives, something that was left out of this ERDC report.

A December 2018 Coastal & Hydraulics Laboratory (CHL) produced a report for USACE with the purpose of analyzing shoreline change along the northern end of Plum Island with respect to present and historical engineering actions (Tyler and Beck, 2018). The CHL study did provide some review of recent

historical trends in shoreline change as part of the overall data review. It employed a shoreline change analysis using historic shorelines and determined that USACE recent jetty repairs in 2013 may have amplified pre-existing morphology changes, but there is "no discernable causal relationship between the jetty rehabilitation and recent erosion." While the wording of this finding reflects the results of USACE analysis, the authors failed to acknowledge the limited scope and other shortcomings of their analysis that led directly to their conclusions. For example, the presentation of recent data by USACE (see Figure 2.1) indicates that the Reservation Terrace shoreline began to erode around 2008, prior to initiation of the South Jetty repair effort. However, data points from this study are only available in 2008 and 2013, where the presentation of the data draws a straight line between pre-construction and post-construction data points. This results in the *appearance* that erosion of Reservation Terrace began prior to the jetty rehabilitation, but this is only an artifact of the limited data. Other information indicates relative stability and/or accretion of Reservation Terrace up until jetty repairs were initiated in 2012, as shown in Figure 2.2. Further, USACE report makes a claim that erosion patterns for the Reservation Terrace shoreline are on a similar cyclical pattern to the erosion 'hotspot' further south on Plum Island, with little to no basis or reasoning for the claim. To effectively assess shoreline change in recent years, it is more appropriate to utilize all available data sets. Several LiDAR sources exist for this section of shoreline (e.g., 2010, 2011, 2014, 2015; see Appendix C) to assess morphology changes on the northern end of Plum Island, where example results are shown in Figure 2.2. From this more robust spatial data set, it appears that the shoreline of Reservation Terrace was stable until the jetty repairs were initiated and rapid erosion of the shoreline occurred following the repair efforts. Based on this LiDAR data set, there appears to be a causal link between the jetty rehabilitation and recent erosion.

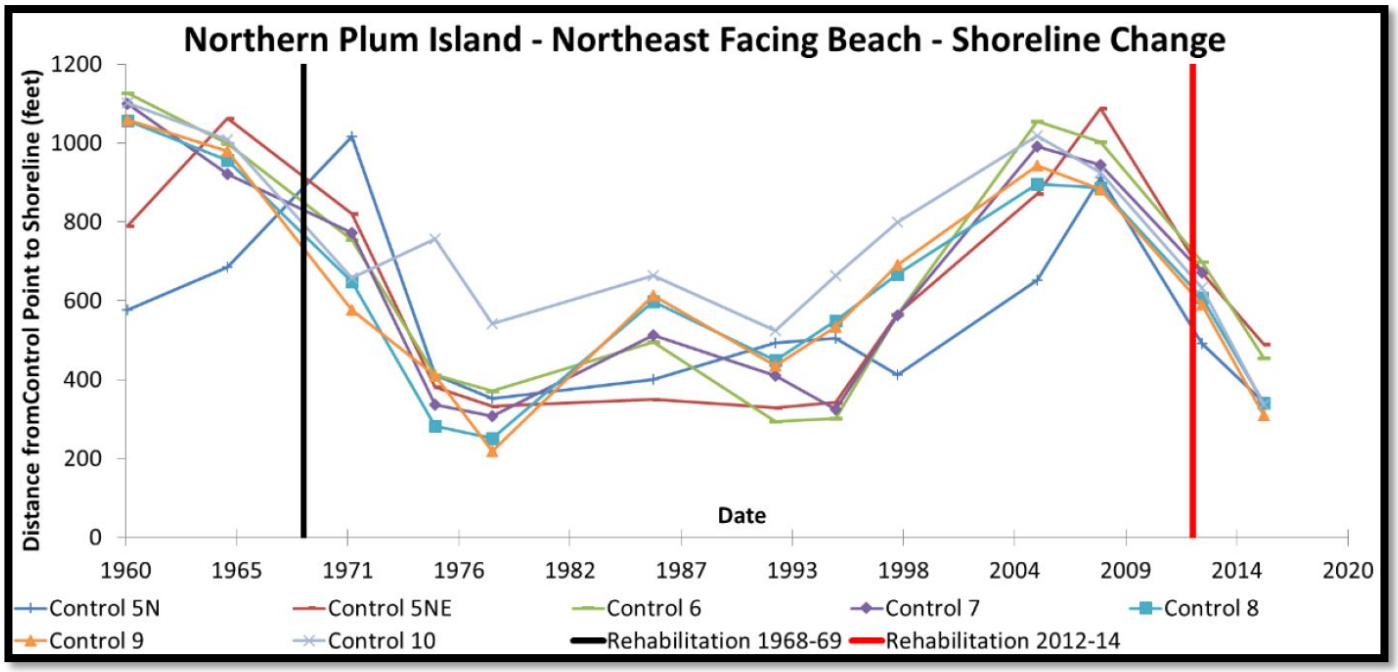

Figure 2.5 Shoreline changes along Reservation Terrace shown in Figure 5 of Tyler and Beck (2018), where it appears that shoreline erosion is initiated prior to the most recent jetty rehabilitation efforts.

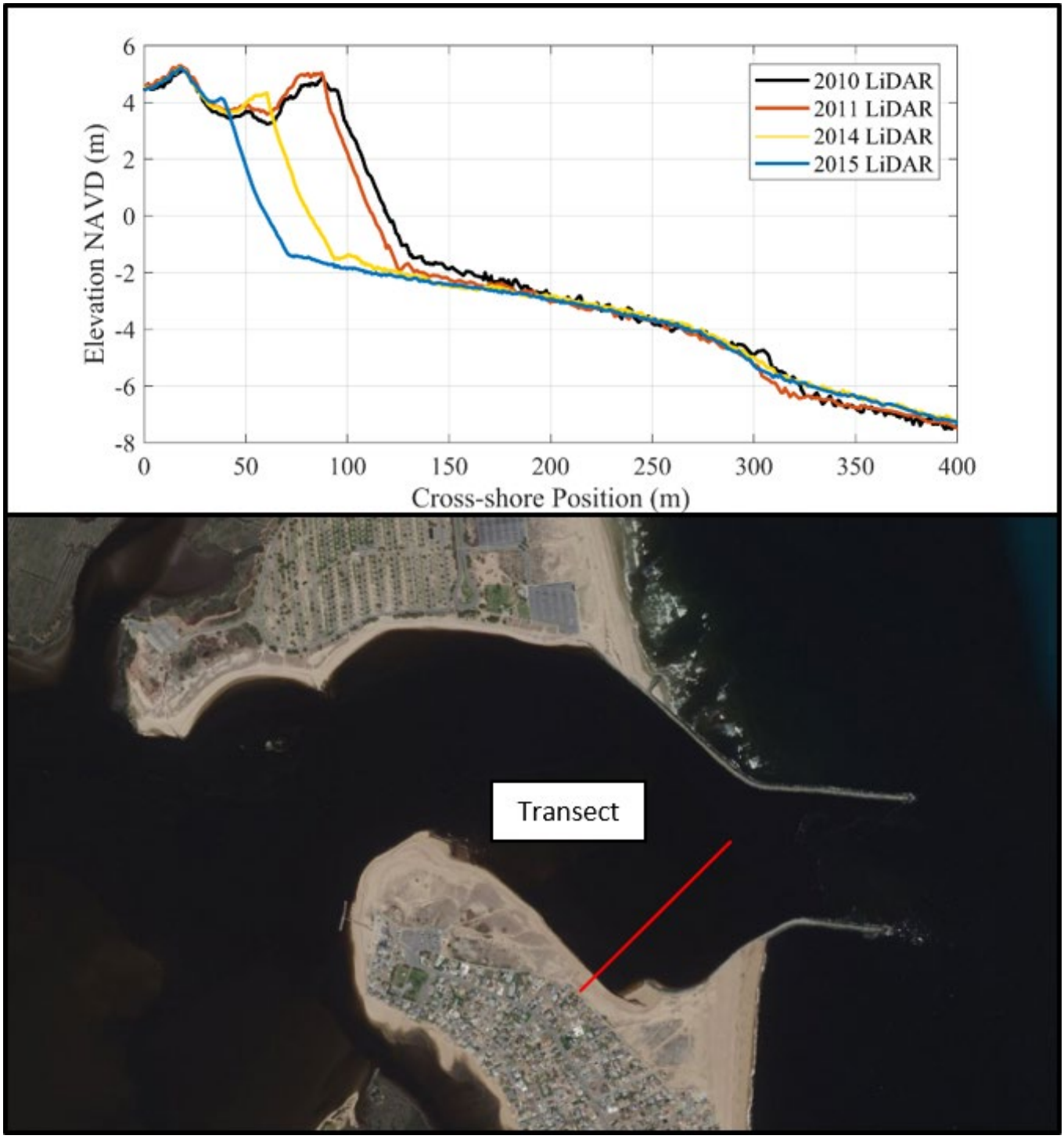

Figure 2.6 Elevation profile of LiDAR transects from 2010, 2011, 2014, and 2015 located across Reservation Terrace. Erosion of the profile accelerates as losses increase from 20 feet per year (2010 to 2011), to 30-40 feet per year (2011 to 2014) and finally 70 feet per year (2014 to 2015).

3.0 EXISTING CONDITIONS

The evaluation of existing conditions for this study incorporated shoreline change analysis, historical structure information, available state and local maps/plans of resource areas, and existing wave refraction modeling output. A description of any unique features of each region was provided that included a description of the on-going coastal processes that continue to shape the shoreline.

3.1 Shoreline Stabilization Structures

The Massachusetts Department of Conservation and Recreation Office of Waterways evaluated shoreline stabilization structures in 2013 to identify the state's vulnerability to storm damage. The structures were categorized by their type and by their structural condition based on a preliminary field assessment. Structures were rated at grades of A through F, with A indicating that the structure did not require any maintenance, repair, or rehabilitation and would not be expected to experience damage during a major coastal storm event, and F indicating that the structure required complete reconstruction and would provide little to no protection from a major coastal storm event. The evaluation was confined to public structures and structures of unknown ownership, public stabilization structures are shown in Table 3.1.

Ownership of structures was determined based on assessor maps and research at the local, state and federal levels. Where there was indication of public work on a structure on Town land or on private property, the structure was presumed to be Town owned. Where the structure was on state property, the structure was presumed to be state owned. Where ownership of the structure was not clear but was located on private property, the structure ownership was defined as unknown. Results of the survey are provided in Table 3.1. Different sections of the project are delineated in Figure 3.1 to distinguish key areas, public and private shoreline stabilization structures, and barrier beach/Area of Critical Environmental Concern (ACEC) delineations.

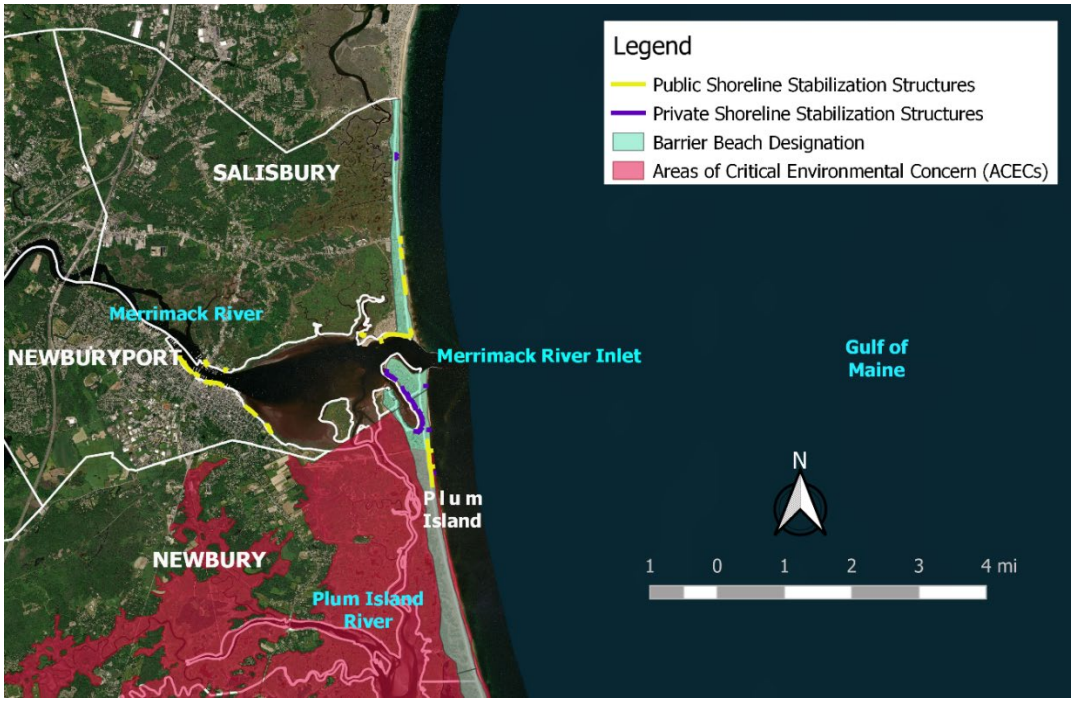

Figure 3.1 Aerial map of the project area, showing key areas, public and private shoreline stabilization structures, and barrier beach/ACEC delineations. Town boundaries also are provided.

Table 3.1 Shoreline stabilization structure inventory. (Source: Bourne Consulting Engineering, 2013)

	Total	A	B	C	D	F	Total Length (ft)
Salisbury							
Bulkhead/Seawall	2		1	1			2,314
Revetment/Seawall	2		2				731
Revetment							
Breakwater							
Groin/Jetty	5		2	3			574
Coastal Dune	4		1	1	2		5,715
Coastal Beach	2	2					162
Newburyport							
Bulkhead/Seawall	11	1	1	8	1		2,585
Revetment/Seawall	1			1			906
Revetment	6	1	3	1	1		2,522
Breakwater							
Groin/Jetty	4			1			4,341
Coastal Dune	3						259
Coastal Beach							
Newbury							
Bulkhead/Seawall							
Revetment/Seawall							
Revetment							
Breakwater							
Groin/Jetty	3			1	2		484
Coastal Dune	1			1			3,390
Coastal Beach	3	1		1	1		970
North Shore (Total)							
Bulkhead/Seawall	13	1	7	5	0	0	4,899
Revetment/Seawall							1,637
Revetment	7	0	6	1	0	0	2,522
Breakwater	0	0	0	0	0	0	0
Groin/Jetty	6	0	3	2	1	0	5,399
Coastal Dune	4	0	1	2	1	0	9,364
Coastal Beach	4	2	2	0	0	0	1,132

3.2 Storm Damage History

To identify stretches of beach that are threatened, Applied Coastal analyzed repetitive loss data. FEMA defines a repetitive loss property as any insurable building for which two or more claims of more than $1,000 were paid by FEMA NFIP (National Flood Insurance Program) within any rolling ten-year period, since 1978. Repetitive loss property data was obtained from FEMA NFIP from 1978 to 2018; the information in the dataset included: the location/address of the properties, number of FEMA claims, the

associated claim dates and claim amounts. It is acknowledged that the repetitive loss data does not include all claims to FEMA and does not take into account damages that property owners decided to not claim; however, the data gives an indication of the spatial distribution and the relative scale of damage costs. Figure 3.2 and Figure 3.3 show the spatial distribution of repetitive loss properties along Salisbury Beach and Plum Island respectively. To maintain confidentiality, the exact locations of the repetitive loss properties are obscured. These properties are typically damaged when a storm surge coincides with a high tide and storm wave runup reaches properties and potentially damages structures. Erosion of the beach out in front of properties accelerates the process by lowering the profile and allowing larger waves to propagate closer to shore during storm events for both Plum Island (Figure 3.4) and Salisbury (Figure 3.5).

Figure 3.2 Spatial distribution of FEMA repetitive loss properties along Salisbury Beach.

Figure 3.3 Spatial distribution of FEMA repetitive loss properties for Plum Island.

Figure 3.4 Example photograph looking northward along a heavily eroded Plum Island beach following a January 2008 storm event in which wave runup reached properties along the shoreline.

Figure 3.5 Example photograph looking northward along Salisbury Beach following a March 2018 northeast storm event.

3.3 Reservation Terrace Shoreline

The stretch of beach on the south side of the inlet, referred to as Reservation Terrace has alternated between accretional and erosive periods following jetty installation in the early 20th century. With limited aerial photography and survey data, it is difficult to accurately define years as accretional or erosional. However, it is possible to consider the forcing mechanisms that play a role in shaping the shoreline, and make management decisions based on these mechanisms. Applied Coastal considered each of these mechanisms to identify management responses for the shorelines. These mechanisms include storm waves, tidal currents, and river flow.

During an east directed swell, waves propagate through the inlet and refract towards the northeast facing Reservation Terrace shoreline. The orientation of the waves relative to the shoreline results in a net directed transport to the northwest and some cross-shore directed transport into the inlet. Based on the analysis of recent LiDAR surveys, there appears to be minimal cross-shore transport of sediment (), where the offshore profile shape remains stable. Transport of material generated from waves therefore likely supports the buildup of the spit off of the northern end of Plum Island (Figure 3.6). Applied Coastal also considered ebbing currents, tidally driven or amplified by strong riverine output from the Merrimack River. Model results indicate that the Reservation Terrace shoreline is mostly sheltered from ebbing currents, even during strong riverine flow events. This was apparent during an event in September of 2011 in which there is a distinct separation between the ebbing flow and stagnant water adjacent to the Reservation Terrace shoreline, as shown in Figure 3.7. Alternatively, model simulations were utilized to evaluate conditions both before and after jetty rehabilitation. Figure 3.8 illustrates peak flood currents associated with the conditions before and after jetty rehabilitation, respectively. During a peak flood tide, currents off

of Reservation Terrace reached 3 feet per second post-rehabilitation. A similar simulation with pre-rehabilitation jetty elevations provided results indicating that currents are cut in half by flow passing over the southern jetty. Results from these modeling scenarios are discussed in more detail in section 5 of this report.

Figure 3.6 Aerial photograph (May 4th, 2018) of the northern Plum Island showing the spit generated along the northern end.

Figure 3.7 Sediment plume ebbing through the Merrimack River Inlet in 2011. Note the stagnant water along Reservation Terrace at the top of the photo. The coloration also indicates a lack of mixing between outward river flow and the waters beyond the navigation channel.

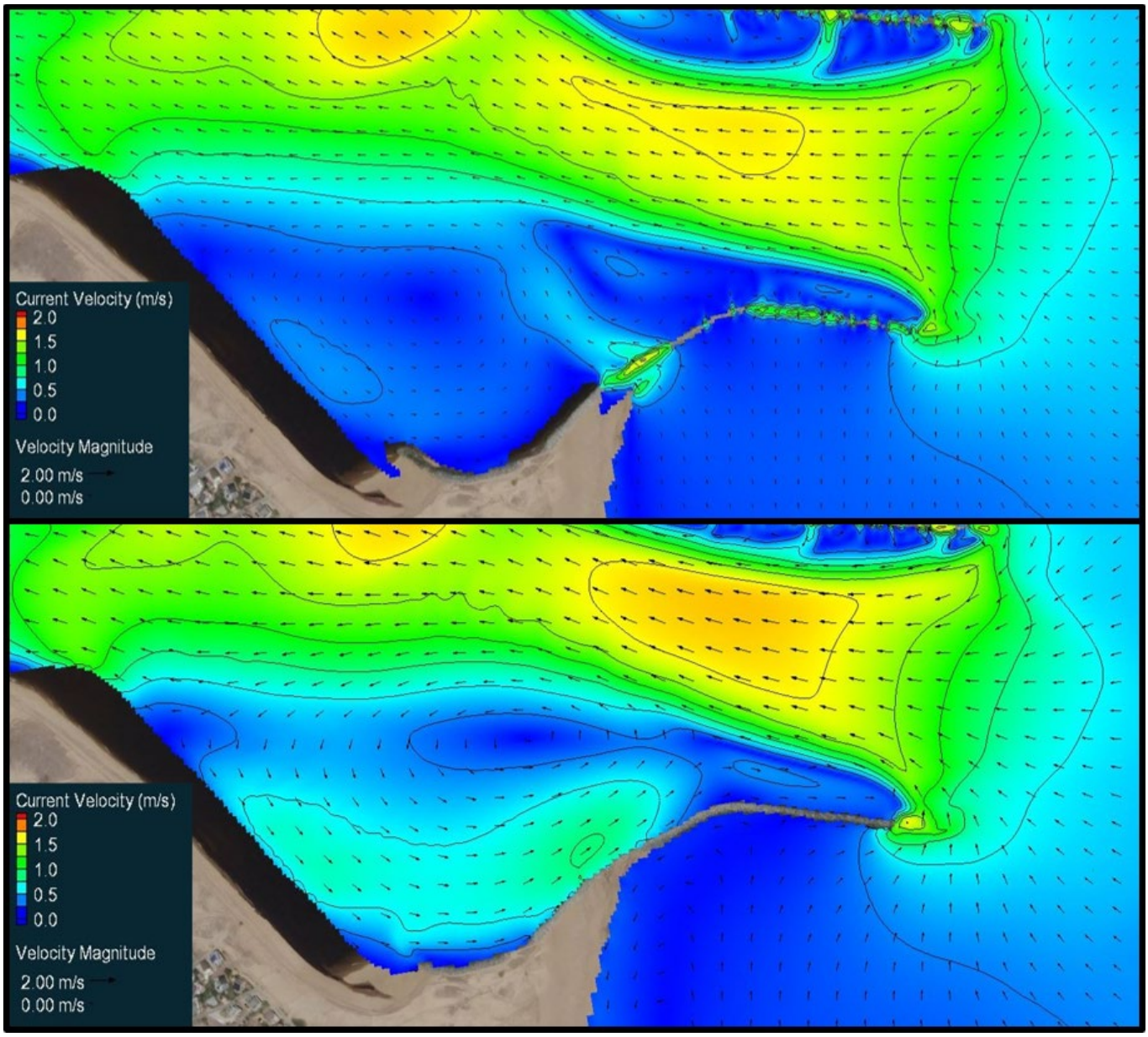

Figure 3.8 CMS Flow results showing the influence the structural condition of the jetties have upon flows into the Merrimack River. The figure shows the same simulation time step at peak flood tide with 2014 bathymetry for both model cases. The elevation data of the jetty in the simulation for the upper plot was edited to include LiDAR (2010) of the jetty prior to USACE rehabilitation in 2013. A circulation gyre develops along Reservation Terrace with currents approaching 0.85 m/s (2.8 ft/s) when the jetty prevents flow through the structure.

3.4 Erosion Hotspot

Previous morphology studies discussed in Section 2.1 associated the erosion hotspot along the Plum Island shoreline with breaks in the bypass bar. However, the mechanisms behind erosion generated by bar breaks have not been studied in detail (Kraus and Galgano, 2001). Fallon (2016) developed a conceptual model for understanding the erosion hotspot, following some preliminary theory developed in the 1970's (Hubbard, 1975; Wentworth, 1969). The specific mechanisms that control the observed

erosional hotspot generation and migration were not quantified in this previous work. From the perspective of coastal processes, the concept of wave refraction altering sediment transport direction, especially at the south end of the bar system is well-documented by observations. Nearshore refraction and breaking of waves along the bar are apparent in Figure 3.9. In addition to wave refraction in the vicinity of the various bar breaks, the modeling analysis included in Sections 4 and 5 investigated the influence of alongshore currents generated during storm events as an additional mechanism that could generate erosion hotspots along this shoreline.

Figure 3.9 Aerial of the ebb tidal delta and bypass bar, with breaking waves outlining the general shape of the feature.

3.5 Sediment Budget

To the extent of practicability, a preliminary sediment budget has been developed based on the availability of data. The accuracy of the sediment budget is limited due to the general lack of long-term survey data for the beach systems surrounding the inlet, as well as the uncertainties related to sediment sources for shoaling within the Merrimack River entrance (i.e. is the shoaling caused primarily by riverine sediments or beach sediments). Within the context of available data, generalized sources and sinks were evaluated to develop an overall sediment budget for the system (Table 3.2).

To determine annual erosion volumes, a simple shoreline response equation (Dean, 2002) was used

$$\Delta y_0 = \frac{V}{h_0 + B}$$

where Δy_0 is the shoreline change, V is the change in volume, h_0 is the breaking wave height offshore, and B is the berm elevation. These cross-shore erosion volume estimates supplemented alongshore transport estimations developed from the calibrated shoreline change model. The combination of these two methods of transport were used to develop the generalized annual sediment budget, and a summary is included in Table 3.2.

Beginning at the northern end of the project area in Salisbury, there is a general southerly directed alongshore transport. The transport direction on a daily basis will primarily depend on wave energy and direction. However, for the purpose of this exercise, the net transport was considered. Smaller nourishments on the order of 1,000 to 10,000 cubic yards along the Salisbury shoreline modify the magnitude of these transport rates. The alongshore transported sediment makes its way south towards the north jetty. As the transported sediment migrates around the north jetty, there is a divergence, where some of the material enters the inlet, and the rest follows the bypass bar.

There is an unquantified exchange in sediment between the bypass bar and the inlet throat. The Merrimack River and estuarine system supplies an unknown volume of sediment to the system, which makes for difficulty in quantifying the annual exchange. There is also transport along Reservation Terrace, which has primarily eroded in the past seven years following jetty rehabilitation. Some of this material that erodes along Reservation Terrace settles at the Northwest tip, forming a spit. Dredging operations within the inlet that average 38,000 cubic yards per year will remove sediment from the system.

As material moves along the bypass bar, there is some exchange with the shoreline. The notable exchange point is at the southern end of the bypass bar. This location represents a sediment transport nodal point at which net annual transport diverges north and south and results in an erosion hotspot. The only sediment supply for this section of shoreline are nourishments, with the only recent significant nourishment project occurring in 2010. Approximate sediment transport pathways and values (thousands of cubic yards transported annually) are included in Figure 3.10.

Table 3.2 Sediment sources and sinks for each region.

Region	Sources	Sinks
Salisbury	• Nourishments • Alongshore transport from the north (seasonal)	• Transport to the south • Cross-shore erosion
Reservation Terrace & Inlet	• Nourishments • Riverine deposition • Salisbury erosion from the north • Plum Island erosion (when south jetty is “leaky”)	• Cross-shore erosion into inlet • Dredging of inlet
Inhabited stretch of Plum Island	• Nourishments • Nearshore bar onshore migration	• Transport to the south at nodal point • Cross-shore erosion (Critical at the erosion hot spot) • “Leaking” of sediment across south jetty

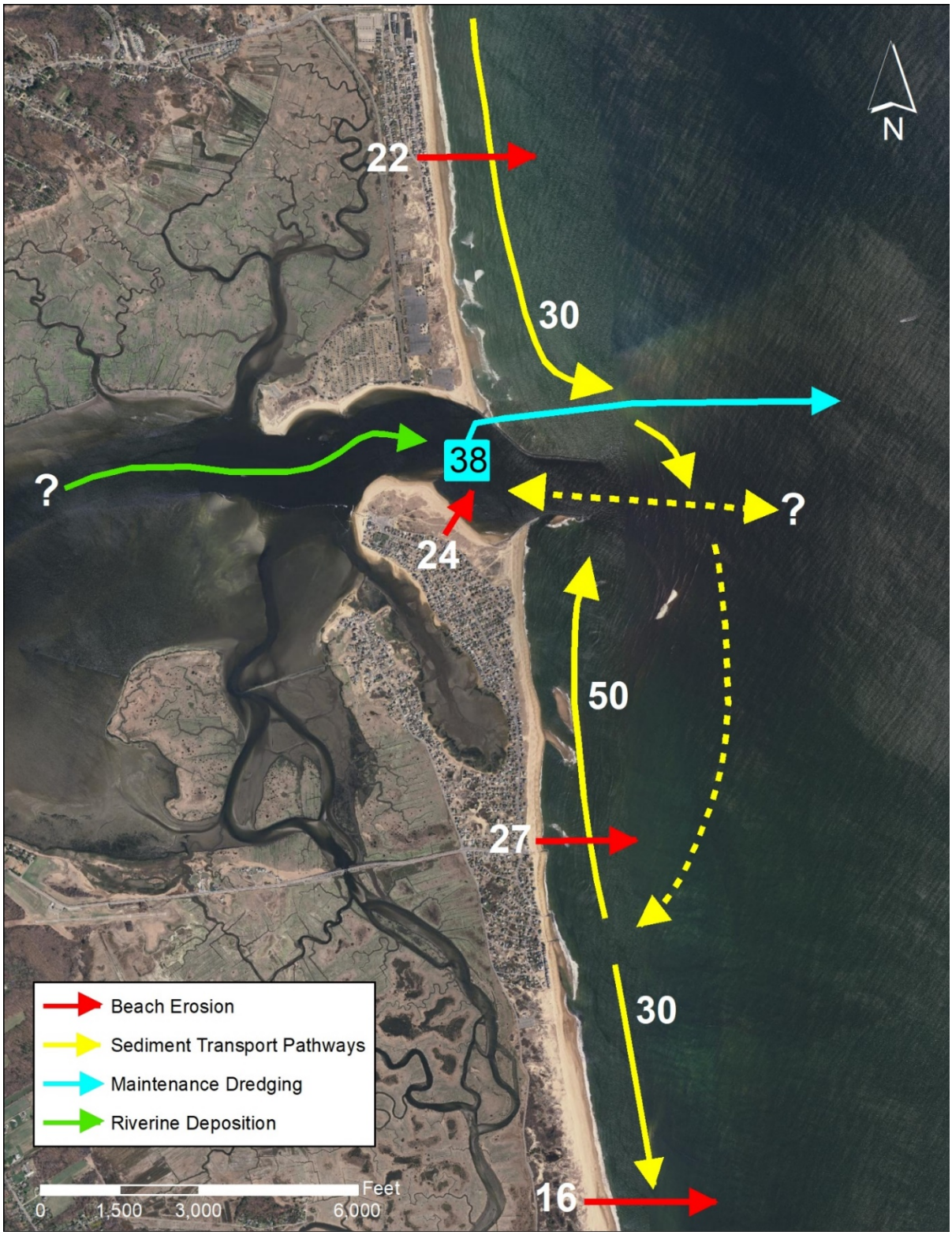

Figure 3.10 Sediment transport pathways along the ocean facing upper north shore coastline. Numbered values represent thousands of cubic yards transported along the pathway annually. Pathways with a question mark indicate uncertainty due to a lack of available data.

4.0 ANALYSIS & ASSESSMENT OF COASTAL PROCESSES & SEDIMENT TRANSPORT

A shoreline modeling analysis was performed to better understand the coastal processes affecting the sediment transport dynamics both north and south of the Merrimack River inlet. The analysis includes the 3.7-mile shoreline up to the Massachusetts and New Hampshire border to the north and 4.5 miles south of the inlet are included in the study (Figure 1.1). This 43,296-foot long shoreline segment features the jetties protecting the Merrimack River inlet sides, in addition to several stone groins south of the inlet.

To assess the coastal processes affecting sediment transport patterns, forcing conditions for the numerical models were developed based on historical data. Waves provide the driving forces governing the observed changes in the position of the study shoreline, over time. Shorter period wind waves are generated locally in the Gulf of Maine, with longer period wave energy propagating from fetches that extend into the open Atlantic Ocean. To determine the distribution of wave energy and the direction of waves approaching the shoreline, a wave refraction analysis was performed. This analysis computed the nearshore wave climate of the study reach based on wind and offshore wave data. The wave modeling predicted the major effects of long-term average wave conditions on the beach and provided the basis for determining trends in sediment transport. The nearshore wave climate developed by this modeling was utilized to drive a shoreline change/longshore sediment transport model. Once completed, the shoreline model was used to evaluate engineered alternatives.

The transport of beach sediments along the project shoreline is induced by complex wave patterns and can be determined using empirical relationships that describe sediment transport potential. Coded as a computer model, these empirical methods can be used to obtain an understanding of existing coastal processes, and are verified through comparison to field measurements. Establishing a model of existing conditions allows for subsequent analyses of proposed nourishment alternatives for a shoreline.

4.1 Wave Modeling

The sediment transport calculations depend upon a long-term wave data record. Ideally, this wave record would come from a data buoy stationed offshore of the site being modeled. In the absence of such a source of long-term data, there are few other reliable options for retrieving wave data. For sites located on the open coast, simulated long-term wave records are available through the Wave Information Study (WIS) conducted by the U.S. Army Engineer Waterways Experiment Station (WES). The WIS program has generated hindcast wave data for waves propagating from open ocean, through the use of computer simulations, for many sites along the U.S. coast.

For the shoreline north and south of the Merrimack Inlet, open ocean exposure increase the potential for sediment transport and thus erosion. Prominent features offshore of the shoreline include the Isle of Shoals, Hampton Shoals, and a periodic sandbar. Cape Ann shelters the study area from a portion of the incident wave energy from the south, and the shoreline positioning to the north limits much of the incident wave energy from the northerly directions. Because it was not initially known what the contribution offshore waves made to sediment transport at the study shoreline, the wave climate was estimated using a method that incorporated offshore waves and locally generated wind waves.

A three-part procedure was followed for the generation of wave input for the sediment transport analysis. First, the long-term WIS wave and wind hindcast data located directly offshore of the Merrimack River Inlet (Figure 4.1) was retrieved and processed. Second, the processed wave and wind data were used as inputs into the two-dimensional wave transformation model SWAN. Third, output from this program was then used to generate the wave input record used in the sediment transport calculations.

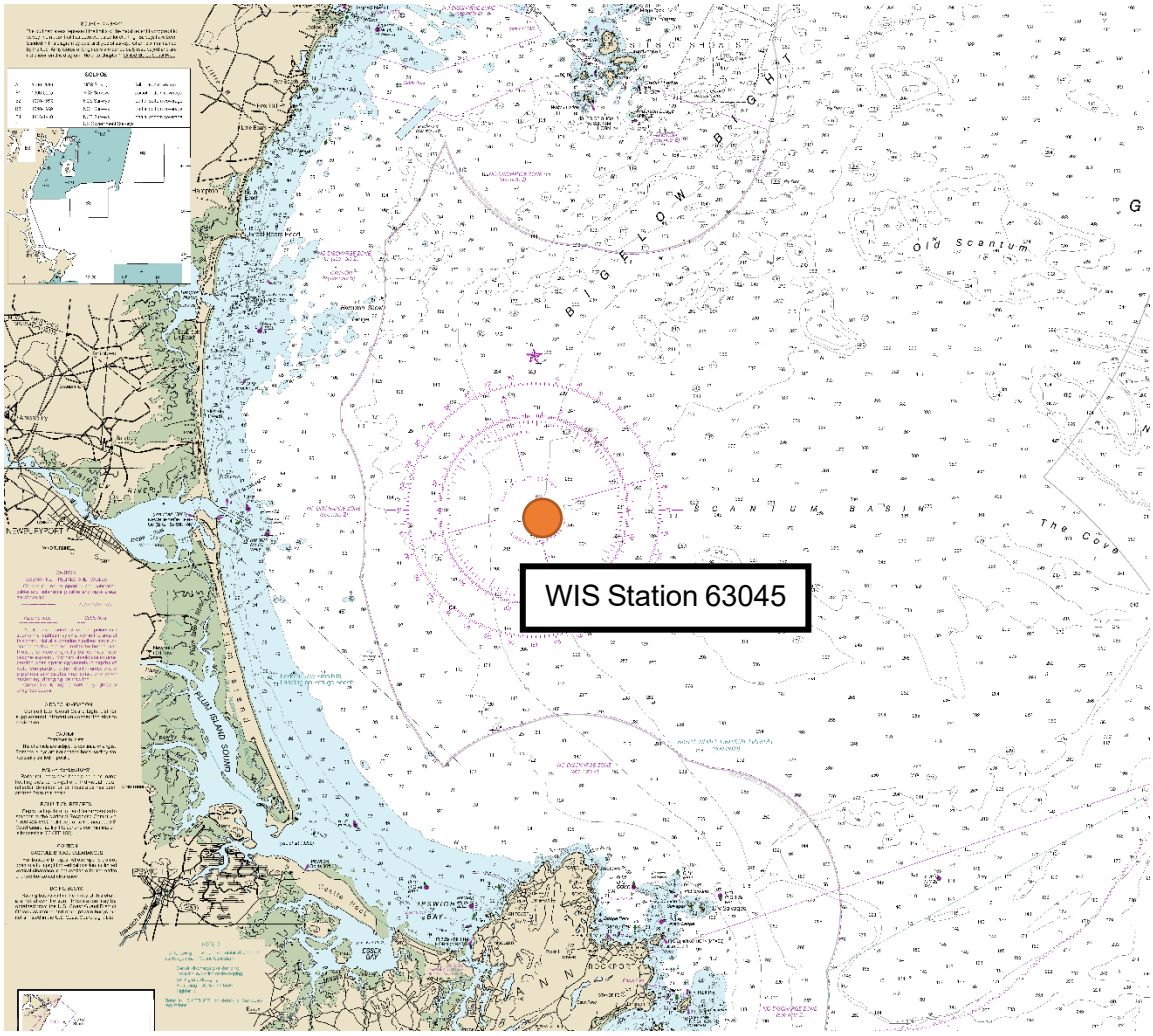

Figure 4.1 Detail of NOAA chart 13278 (Cape Ann to Portsmouth) showing the locations of the WIS hindcast station (63045) and the north shore study shoreline.

4.1.1 Wave and Wind Data

For this study, wave conditions were generated using the wind and wave data available from USACE WIS hindcast database, at station 63045 (see Appendix C). The WIS data were used to develop offshore wave boundary conditions as well as the winds applied to the surface of Gulf of Maine. The WIS has a record that spans the 35-year period between January 1980 through December 2014.

The entire wind and wave records from the WIS hindcast are presented in Figure 4.2 and Figure 4.3, respectively, as compass rose plots which show magnitude and percent occurrence by compass sector. From the hindcast, winds most frequently blow from the south-southwest (SSW), with a percent occurrence of 9.6%. For sectors approaching the north shore shoreline (north through south) winds blow 43.1% of the time. From all direction sectors, wind speeds are greater than 10 knots 52.1% of the record and greater than 25 knots for 3.5% of the record.

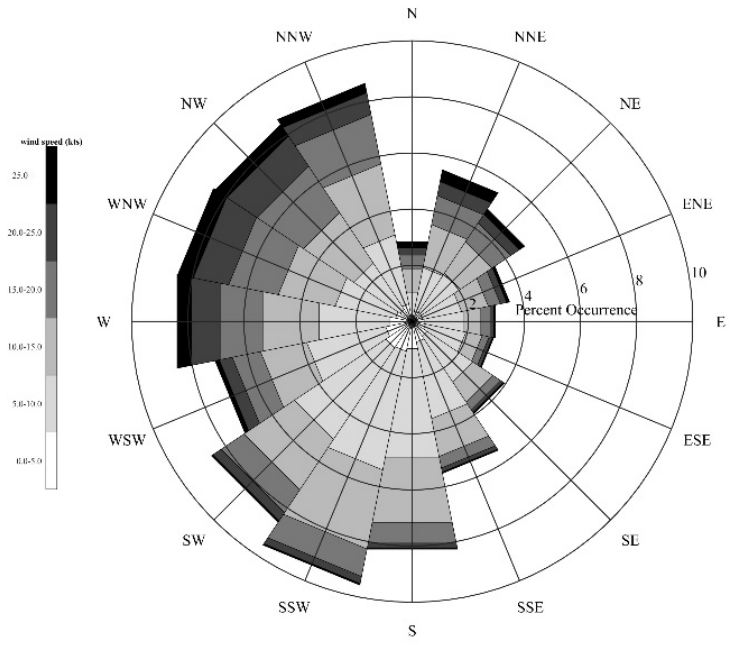

Figure 4.2 Wind rose of data from the WIS hindcast station 63045, for the 35-year period between January 1980 and December 2014. Direction indicates from where wind was blowing. Length of individual segments indicate magnitude of wind speeds. Radial length of each segment indicates percent occurrence over the total duration of the data record.

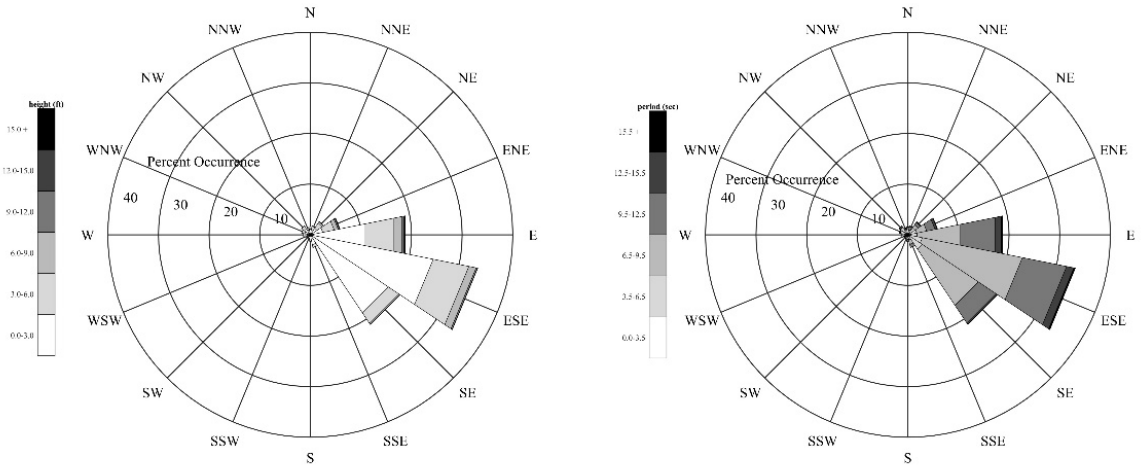

Figure 4.3 Wave height and period for hindcast data from WIS station 63045 for the 35-year period between January 1980 and December 2014. Direction indicates from where waves were traveling, relative to true north. Radial length of segments indicates percent occurrence for each range of wave heights and periods. Combined length of segments in each sector indicate percent occurrence of all waves from that direction.

For the wave data of the WIS hindcast record, the predominant sector is from the east-southeast (ESE). Waves propagate from this direction 33.7% of the time. The second-most frequently occurring sector at this station is southeast (SE), which occurs 21.3% of the time. Most of the waves from the east

(E) sector (approximately 19.1% of the total record) have significant wave height between 3.3 and 9.8 feet. In some instances, waves from the E exceeded 18 feet.

To develop the input conditions for the wave model, the wave data from the WIS record were binned by 22.5-degree compass sector and by magnitude, as presented in Table 4.1. Each hourly WIS record includes parameters that describe the wave conditions (i.e., wave period, T_p; wave height, H_s; and direction, θ). For each separate compass sector, the hourly events from the wave record were divided into top, middle and bottom bins, based on significant wave height. The average value of significant wave height was chosen as the value for each bin. For each separate sector, this binning method resulted in two more frequently occurring wave cases (bottom and middle bins) that represent more common conditions and one less frequently occurring bin (top bin) that represents rarer storm conditions. A total of 306,814 total hourly time steps of the WIS record were sorted in this fashion.

The WIS hindcast record also was used to determine the offshore wind input conditions. Wind conditions for each wave case were determined by the wind data concurrent with the wave records. Average wind speeds for each wave case were selected as the input conditions. Wind direction was determined as the vector average direction of all wind cases occurring with each wave case. This method of sorting the wind data determines the average wind conditions that correspond to each binned wave case.

Twenty-seven separate model cases (i.e., three wave cases from each of eleven compass sectors) were developed by this processing of the wind and wave data of the WIS record, Table 6.1. The nine compass sectors from north (N) to south (S) include all winds that generate waves to drive sediment transport along the study shoreline. The percent occurrence of each separate case is determined using the number of hourly records from the WIS hindcast that fall into each bin, divided by the total number of wave records in the entire 35-year record.

4.1.2 Bathymetry Data and Grid Development

In addition to the wind and wave boundary conditions specified for each of the wave cases, bathymetry and several model parameters must be specified. The model parameters describe the extent and resolution of the computational mesh (separate from the bathymetry grid) including nested grids (smaller refined grids with greater detail), the directional and frequency resolution of the wave spectrum, and wave physics (e.g., breaking, wave-wave interactions).

The SWAN model developed for the project site used a coarse grid with 164-foot (50-meter) spacing for the region including the offshore area of the Gulf of Maine, including Cape Ann to the south and the Isle of Shoals to the North (Figure 4.4), and two nested fine-scale 16.4 foot (5-meter) grids. The upper grid covers the shoreline to the north of the inlet and the lower grid covers the shoreline to the south of the inlet.

The coarse grid was used to propagate offshore waves developed from the analysis of the WIS hindcast record, and also generate wind-waves within several km of the shoreline. The nested fine-scale mesh serves to provide highly-detailed wave information at either shoreline of interest, which were used as input conditions for the shoreline change model of the study shoreline. As executed, spatially varying model output from the coarse grid (at points that correspond to nodes along the fine grid open boundary) is used as the boundary condition for the fine scale grid model runs, therefore the refined grid results are truly nested within the coarse grid simulations.

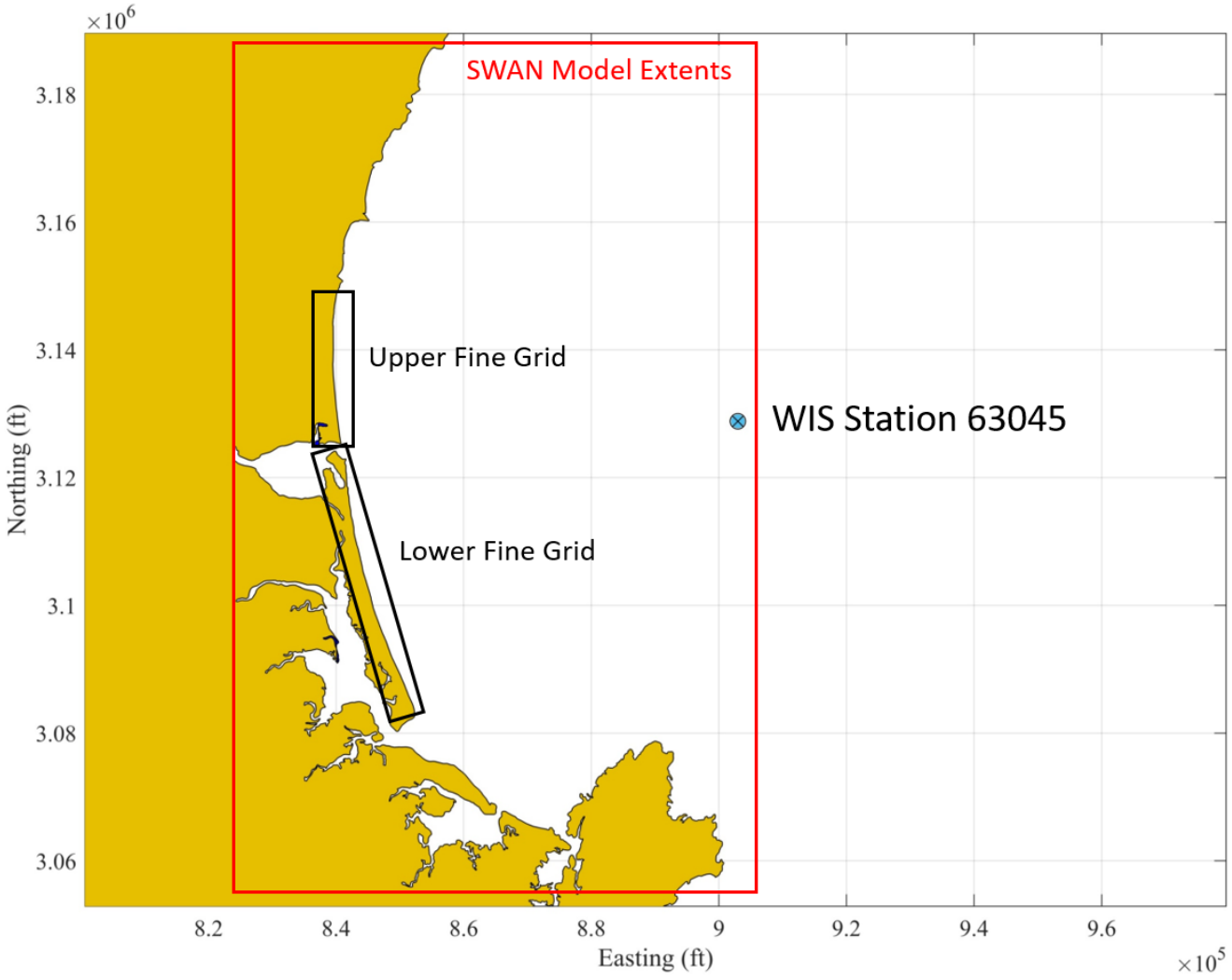

Figure 4.4 Map showing wave model grid limits and bathymetry, for the coarse model grid of the Gulf of Maine, and the limits of the fine-scale model grid for both Salisbury Beach and Plum Island.

The coarse grid is made up of 370,595 computational cells with a spacing of 164 feet (50 meters). The x-axis of the grid is 11.2 nautical miles (20.8 km) or 415 cells wide. The y-axis of the grid is 24.1 nautical miles (44.7 km) or 893 cells long. The y-axis is oriented due north. The greatest depth in the coarse grid domain is -335 feet NAVD (-48 meters). The upper fine-scale 16.4-foot (5 meter) grid is made up of 690,274 total cells. The x-axis is oriented along the Salisbury Beach Shoreline, and has a total length of 4.8 nautical miles (9.0 km). The y-axis is oriented along the compass heading of 86.4 degrees. The y-axis has a total cross-shore length of 1.0 nautical miles (1.9 km). The lower fine-scale 16.4-foot (5 meter) grid is made up of 883,742 total cells. The x-axis is oriented normal to the Plum Island shoreline, and has a total length of 6.0 nautical miles (11.2 km). The y-axis is oriented along the compass heading of 79.4 degrees. The y-axis has a total cross-shore length of 1.1 nautical miles (2.0 km). The National Ocean Service (NOS, 2018) was the main source of bathymetric data used to create the grids. Additional high-resolution elevation data were available from a 2013-2014 LiDAR flight of the area by USACE which includes the upland of the study area. All elevation data were transformed to the NAVD datum. Figure 4.5 shows the three grids with interpolated LiDAR and NOS survey data.

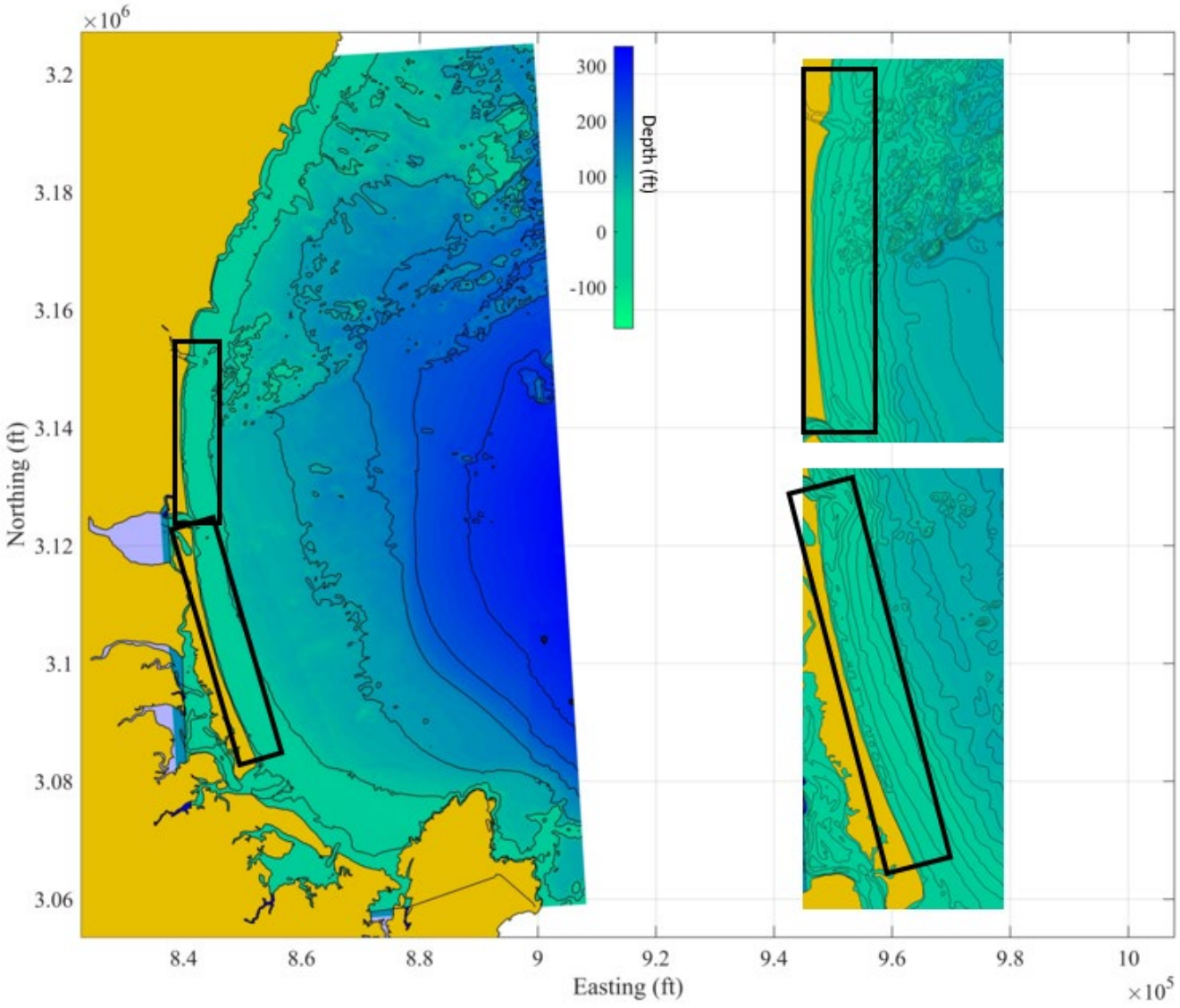

Figure 4.5 Map showing wave model grid limits and bathymetry, for the coarse model grid of the Gulf of Maine, and the limits of the fine-scale model grid for both Salisbury and Plum Island. Contour lines are shown at 40-foot intervals for the left plot 10-foot intervals on the zoomed in figures.

4.1.3 Swan Model Development

As locally generated and offshore wave components propagate into shallower water near shore, the height of the shoaling waves will change, and they will gradually change direction to conform to the bathymetry in that area. In order to estimate how waves will change as they grow under the influence of winds blowing across the surface of the Gulf of Maine and towards the shoreline, the two-dimensional wave transformation program SWAN was used. As discussed previously, wind data from the NOAA buoy and wave data from the WIS hindcast were used as boundary input to the runs of SWAN.

Developed at the Delft University of Technology of the Netherlands, SWAN Cycle III version 41.20 is a steady state, spectral wave transformation model (Booij et al., 1999). Two-dimensional (frequency and direction vs. energy) spectra are used as input to the model. SWAN (an acronym for Simulating Waves Nearshore) is able to simulate wave refraction and shoaling induced by changes in bathymetry and by wave interactions with currents. The model includes a wave breaking model based on water depth and wave steepness. Model output includes significant wave height H_s, peak period T_p, and wave direction θ.

Table 4.1 Wave model input parameters, listed by compass sector and wave height bin (i.e., bottom, middle and top thirds). Listed offshore wave parameters include compass direction θ_o, peak wave period T_o and wave height $H_{s,o}$. Angles are given in the meteorological convention (i.e., from where the wind blows, in compass degrees).

sector		percent occ.	wind angle (degrees)	wind speed (m/s)	θ_o (degrees)	$H_{s,o}$ (feet)	T_o (seconds)
N	bot 1/3	1.3	322.71	8.22	0.02	2.3	6.28
	mid 1/3	0.3	320.59	12.85	0.39	4.5	6.34
	top 1/3	0.005	316.45	18.67	4.81	8.4	6.17
NNE	bot 1/3	1.5	333.95	7.79	22.8	2.5	7.00
	mid 1/3	0.3	336.29	12.93	24.72	5.3	7.06
	top 1/3	0.01	338.38	19.35	25.08	9.7	8.17
NE	bot 1/3	2.7	352.77	7.85	45.83	3.0	7.23
	mid 1/3	0.4	358.66	13.87	47.09	7.2	7.52
	top 1/3	0.02	3.48	20.93	48.27	13.6	9.66
ENE	bot 1/3	5.0	6.26	7.21	68.65	3.4	8.27
	mid 1/3	0.9	14.05	12.86	68.56	8.6	8.93
	top 1/3	0.09	19.67	17.8	69.87	14.9	11.11
E	bot 1/3	17.9	345.34	5.2	92.18	3.3	9.24
	mid 1/3	1.1	30.48	10.07	90.82	9.9	10.69
	top 1/3	0.09	51.11	15.76	89.78	18.2	12.77
ESE	bot 1/3	32.0	213.16	4.49	113.77	2.5	8.71
	mid 1/3	1.7	166.77	7.6	110.68	7.7	10.51
	top 1/3	0.05	84.46	10.25	110.6	13.7	12.32
SE	bot 1/3	20.3	212.19	4.67	130.29	1.9	8.09
	mid 1/3	0.9	212.94	9.86	131.38	5.4	8.51
	top 1/3	0.07	181.56	14.63	130.44	9.8	8.85
SSE	bot 1/3	2.1	220.31	7.17	155.59	2.1	7.41
	mid 1/3	0.4	223.78	11.31	155.69	4.3	7.81
	top 1/3	0.02	230.85	15.64	153.52	7.6	8.87
S	bot 1/3	0.9	231.77	7.3	179.23	1.8	7.02
	mid 1/3	0.4	232.81	10.9	179.13	3.4	7.15
	top 1/3	0.02	247.21	15.3	176.87	6.1	9.05

SWAN is a flexible and efficient program based on the wave action balance equation that can quickly solve wave conditions in a two-dimensional domain using the iterative Gauss-Seidel technique. For this study, the model was implemented using a steady state finite-difference scheme, on a regular Cartesian grid (grid increments in the *x* and *y* directions are equal), though other options are available (including a finite difference formulation using an unstructured mesh). An advantage of the iterative technique employed in SWAN it that it can compute spectral wave components for the full 360-degree compass circle.

The wave spectrum resolution specified for the model runs of both coarse and fine model meshes included the full 360-degree compass circle divided into 72, five-degree segments, with 40 discrete frequencies, between 0.06 and 1.00 Hz (corresponding to periods of between 16.7 and 1.0 seconds). Examples of wave model output are presented in Figure 4.6 for the coarse grid and Figure 4.7 and Figure 4.8 for the upper and lower grids respectively. In these plots the color contours indicate wave height and vectors are used to indicate the direction of wave propagation.

In Figure 4.6, offshore waves with heights of 18.2 feet approach the entrance to the Gulf of Maine in the course grid. The refraction effect of the Isle of Shoals to the north and Hampton shoals just off the Salisbury and Hampton shoreline is evident in this plot. Wave heights at shoreline areas that are more exposed, such as Salisbury Beach and Southern Plum Island, experience wave heights that are greater than 10 feet. At the entrance to the Merrimack River Inlet, even with a wind of 30.7 knots, waves are less than half the wave height at positions further north or south due to the sheltering provided by the bypass bar.

Results plotted for the fine-scale grid for Plum Island (Figure 4.8) show that waves entering the cove area are oriented along its long axis. Wave heights of about 7 feet occur over most of the shoreline, but as waves enter the shallower water along the perimeter of the shoreline they refract and turn normal to the beach. Refraction also causes a reduction in wave height. Further wave height reduction occurs by breaking as the waves roll in to the surf zone at the shoreline.

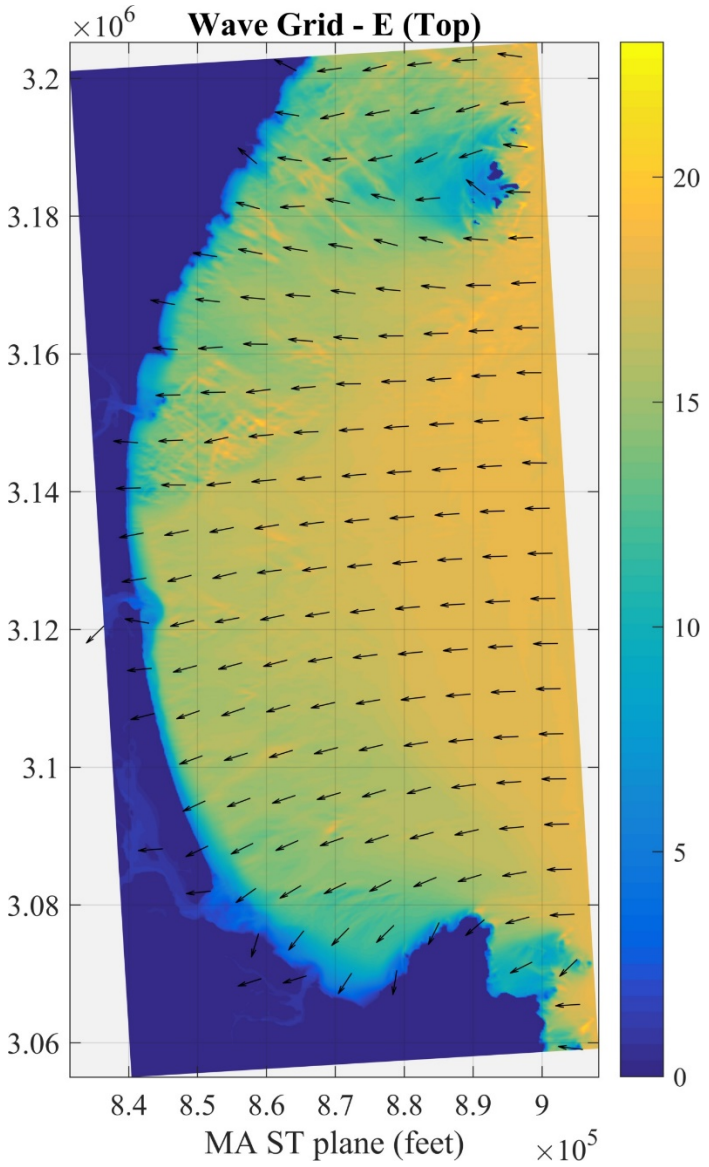

Figure 4.6 Coarse grid output for top E wind case (30.7 knot winds blowing from the South sector, with a 18.2 foot, 10.5 second offshore wave approaching from the South sector). Color contours indicate wave heights (m) and vectors show peak wave direction.

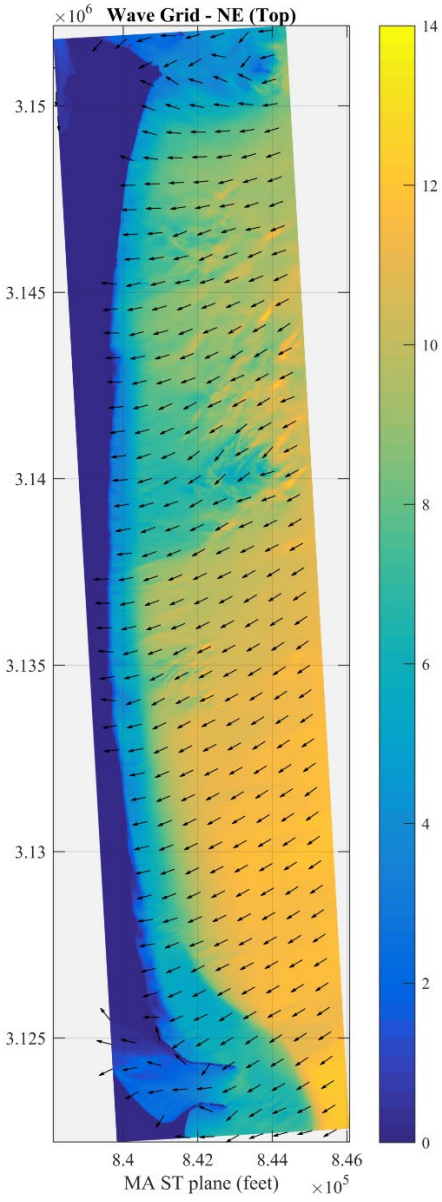

Figure 4.7 Nested fine-scale wave model output for the top Northeast top wind case (Table 3.1). Color contours indicate wave heights (ft) and vectors show peak wave direction.

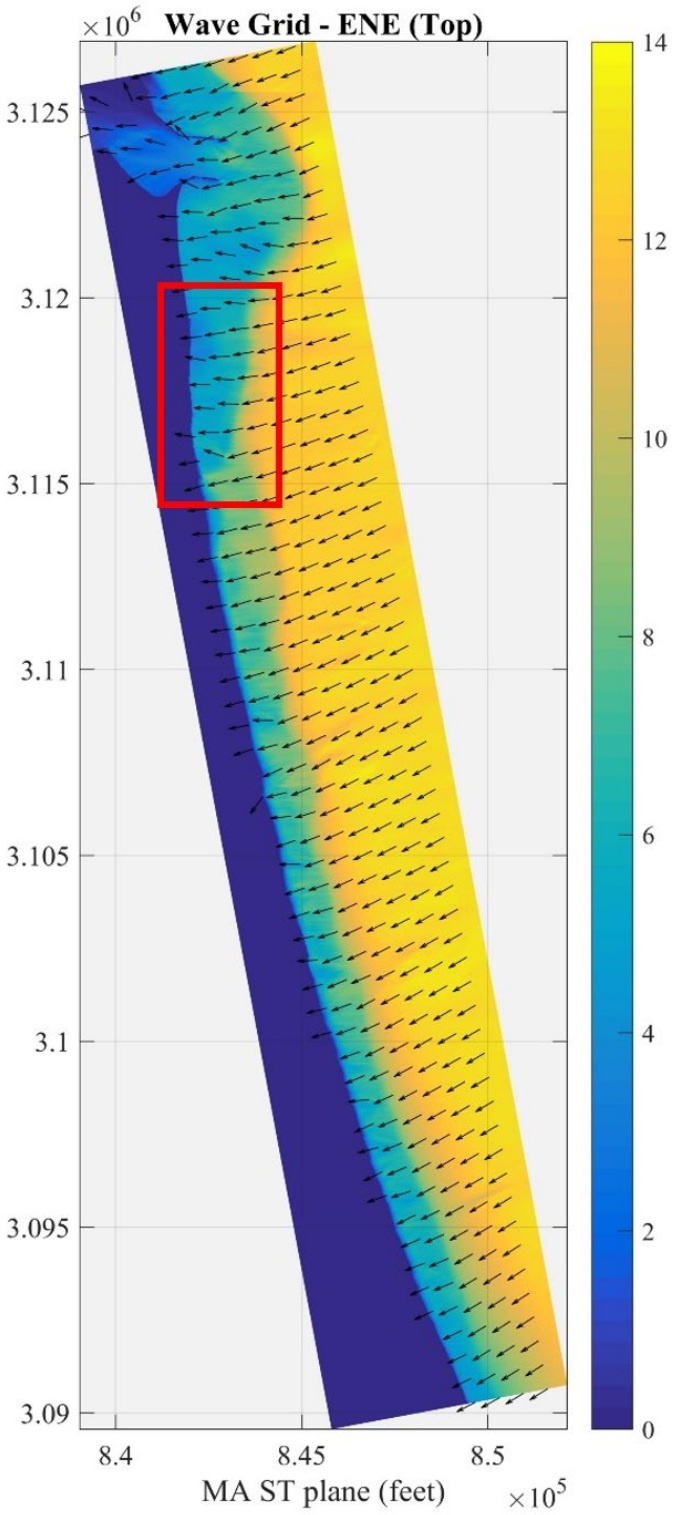

Figure 4.8 Nested fine-scale wave model output for the top East Northeast (ENE) wind case (Table 3.1). Color contours indicate wave heights (ft) and vectors show peak wave direction. Note the refraction of waves around the southern end of the bypass bar (red box), resulting in north-directed transport.

4.2 Shoreline Evolution Modeling

A variety of computational models were employed to study the transport of beach sediment and resulting shoreline change from wave action. The technical sophistication of models ranges from simplified mathematical solutions of equations governing broad physical principles (*analytical* models) to highly complex computer models that simulate natural phenomena contributing to coastal erosion. The most complex computer models (three-dimensional models) require the most detailed input data. The model best suited for studying coastal processes along the upper and lower north shore project limits falls in the middle of this technical range. While simplified analytical models ignore many of the important principles governing shoreline change, the most complex models attempt to simulate the inter-relation of complex physical phenomena not fully understood by scientists/engineers. Thus, a blend of advanced scientific principles with practical engineering assumptions are used in the development of a useful shoreline change model for this analysis.

Shoreline evolution modeling at the north shore was performed using a “one-line” longshore transport computer code. So called “one-line” models simulate the evolution of a shoreline through time, at one specific contour level, e.g. the beach berm crest or mean water level, based on the assumption that the nearshore bathymetry (to the depth of closure used to define the active extent of the beach profile) can be adequately represented by straight and parallel contours. Examples of formulations of this type of shoreline model are very well documented in the literature, e.g., Dean and Dalrymple (2001), Hansen and Kraus (1989).

4.2.1 Sediment Transport Modeling

To properly evaluate natural forces influencing nearshore sediment movement along the ocean-facing beaches, an analysis of coastal processes (primarily waves) governing beach sediment transport was performed. Spectral wave refraction modeling was used to determine how nearshore bathymetry modifies the wave climate along the open ocean beaches of Salisbury, Newburyport, and Newbury. The shoreline limits of the study area are shown on Figure 1.1.

Since this area incorporates the effects of both locally generated wind waves and swell generated offshore in the open North Atlantic Ocean, wave transformation modeling was required to incorporate both components. Wave information used to drive the wave refraction model was developed from locally available wind information (NOAA buoy data), as well as available NOAA and USACE data sets for this portion of the North Atlantic Ocean. Information from the wave modeling was incorporated into a longshore sediment transport model developed by Applied Coastal. Typical of any modeling effort, model results can only be as good as the data utilized for boundary conditions and calibration. For the sediment transport/shoreline change model, appropriate nearshore wave climate, grain size, and historic shoreline change data are required to accurately simulate sediment transport.

Since the purpose of the sediment transport study is to focus on changes to the nearshore regions in the contemporary time-frame, shoreline data used to validate the modeling effort focused on the time period since the 1950s (1952 shoreline). Historic shoreline change data from 2005 and 2015 satellite imagery (Figure 4.9) derived shorelines were utilized to corroborate model results. In addition, Applied Coastal corroborated these data sets with additional shoreline change analysis based on our database of NOAA Topographic Sheets, as well as a review of LiDAR and other data sources. Once calibrated and validated, the shoreline change model can be used to assess sediment transport pathways and delineate littoral cells, determine future migration of the shoreline, provide the basis for a sediment budget, and delineate sources and sinks at the limits of the delineated littoral cells.